ISTITUTO NAZIONALE DI GEOFISICA E VULCANOLOGIA

# Site characterization report at the seismic station IV.INTR – Introdacqua (AQ)

# Report di caratterizzazione di sito presso la stazione sismica IV.INTR – Introdacqua (AQ)

| | |
|---|---|
| **Working Group**<br><br>**Geology:** Marta Pischiutta, Luca Minarelli<br>**Geophysics**: Maurizio Vassallo, Giuseppe Di Giulio, Marta Pischiutta, Alessia Mercuri, Luca Minarelli | Date: December 2020 |
| Subject: **Final report illustrating the site characterization for seismic station IV.INTR** | |

**Convenzione DPC-INGV 2019-21, All.B2- WP1, Task 2:** "Caratterizzazione siti accelerometrici" (Coord.: G.Cultrera, F. Pacor)
**Cite as:** Working group INGV "Agreement DPC-INGV 2019-21, All.B2- WP1, Task 2", (2020). Site characterization report at the seismic station *IV.INTR– Introdacqua (AQ)*. http://hdl.handle.net/2122/14054

**INDEX** **Page**

# INTRODUCTION

In this report we present the geological setting and the geophysical measurements and results obtained in the framework of the 2019-2021 agreement between INGV and DPC, called *Allegato B2: Obiettivo 1 - TASK 2: Caratterizzazione siti accelerometrici (Responsabili: G. Cultrera, F. Pacor)* for the site characterization of station IV.INTR (Introdacqua).

Location and coordinates are reported in Table 1.

**Table 1.**

| CODE | NAME | LAT [°] | LON [°] | ELEVATION [m] |
|---|---|---|---|---|
| IV.INTR | Introdacqua (AQ) | 41.01154* | 13.90460* | 857** |
| ADDRESS | Via Aldo Moro, 25-1, 67030 Introdacqua AQ, Italy | | | |

* Coordinates from ITACA (Nov. 2019) **Elevation from CTR 5k Regione Abruzzo

# A. Geological setting

## A1. TOPOGRAPHIC AND GEOLOGICAL INFORMATION

Topographic information related to the site are reported in Table 2. Table 3 summarizes all available geological maps from literature for geological analyses.

**Table 2.**

| Topography | Description | Topography Class | Morphology Class | EC8 Class |
|---|---|---|---|---|
| | *Flat surfaces, isolated slope and reliefs with slope i<=15° **reliefs with ridge top width much smaller than the base and slope 15°≤i<=30° | *T1 **T3 | R | B |

*Reference table from ITACA (Nov. 2019)

** Reference table from CRISP working group

**Table 3.**

| Geological map | Source | Scale |
|---|---|---|
| **IV.INTR** | Geological map of Italy sheets 369 (Sulmona) | 1:50.000 |
| **IV.INTR** | Geological map of Italy sheets 146 (Sulmona) | 1:100.000 |
| **IV.INTR** | Lithological map of Italy sheets 146 (Sulmona) | 1:100.000 |
| **IV.INTR** | Carta Geologica-Tecnica per la Microzonazione Sismica di Livello 1, Regione Abruzzo, comune di Introdacqua (May, 2020) | 1:5.000 |

In Table 4 Geological and Lithotechnical Units (according to Seismic Microzonation classification; Technical Commission SM, 2015) are described and are concerned to maps of following chapters. The term “original” means the result comes from a preexisting cartography (Table 3); the term “deduced” means the result comes from an interpretation of a preexisting cartography according to the nomenclature of corresponding cartography.

**Table 4**

| **GEOLOGICAL UNITS** | | **LITHOTECHNICAL UNITS** | |
|---|---|---|---|
| Geological map of Italy sheets 369 (Sulmona) | | (MZS) *deduced* | |
| **code** | **description** | **code** | **description** |
| VAP | Verde ammonitico Fm. (Middle Jurassic) | SFLPS | Layered, fractured / weathered bedrock |
| CDI | Calcari diasprigni detritici Fm. (Upper Jurassic) | SFLPS | Layered, fractured / weathered bedrock |
| CRF | Calcareniti a radiolari e resti filamentosi Fm. (Upper Jurassic) | SFLPS | Layered, fractured / weathered bedrock |
| CCF | Calcareniti e calciruditi a fucoidi Fm. (Middle Cretaceous) | SFLPS | Layered, fractured / weathered bedrock |
| Fal | Debris flow (Pleistocene) | GTfd | Unsorted debris flow gravels, mix of gravel, sand and silt. |
| all1 | Unconsolidated sandy gravels (Pleistocene) | GTca | Low-sorted unconsolidated alluvial fan sandy-gravels. |
| Fal | Eluvial and colluvial loosely-consolidated deposits (Olocene) | SMec | Eluvial and colluvial loosely-consolidated silty sands |

## A2. GEOLOGICAL MAP

In Figure 1 Geological Map is reported in a 1km x 1Km square around the station.

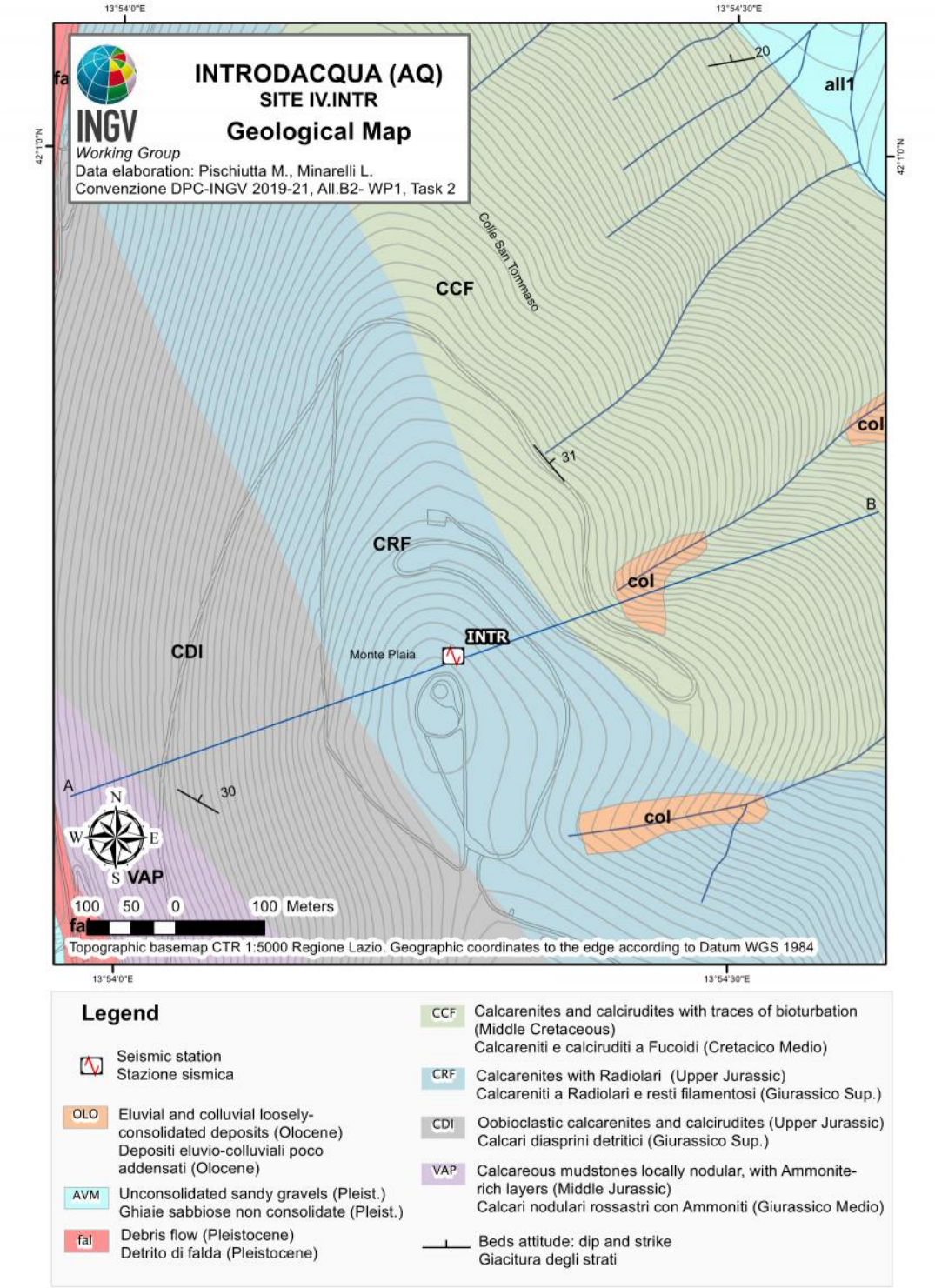


**Figure 1.** Geological map of seismic station IV.INTR, scale 1:5.000. Geological units come from the Geological map of Italy sheets 369 (Sulmona), scale 1:50.000.

## A3. LITHOTECHNICAL MAP

In Figure 2, Lithotechnical Map is reported in a 1km x 1Km square around the station.

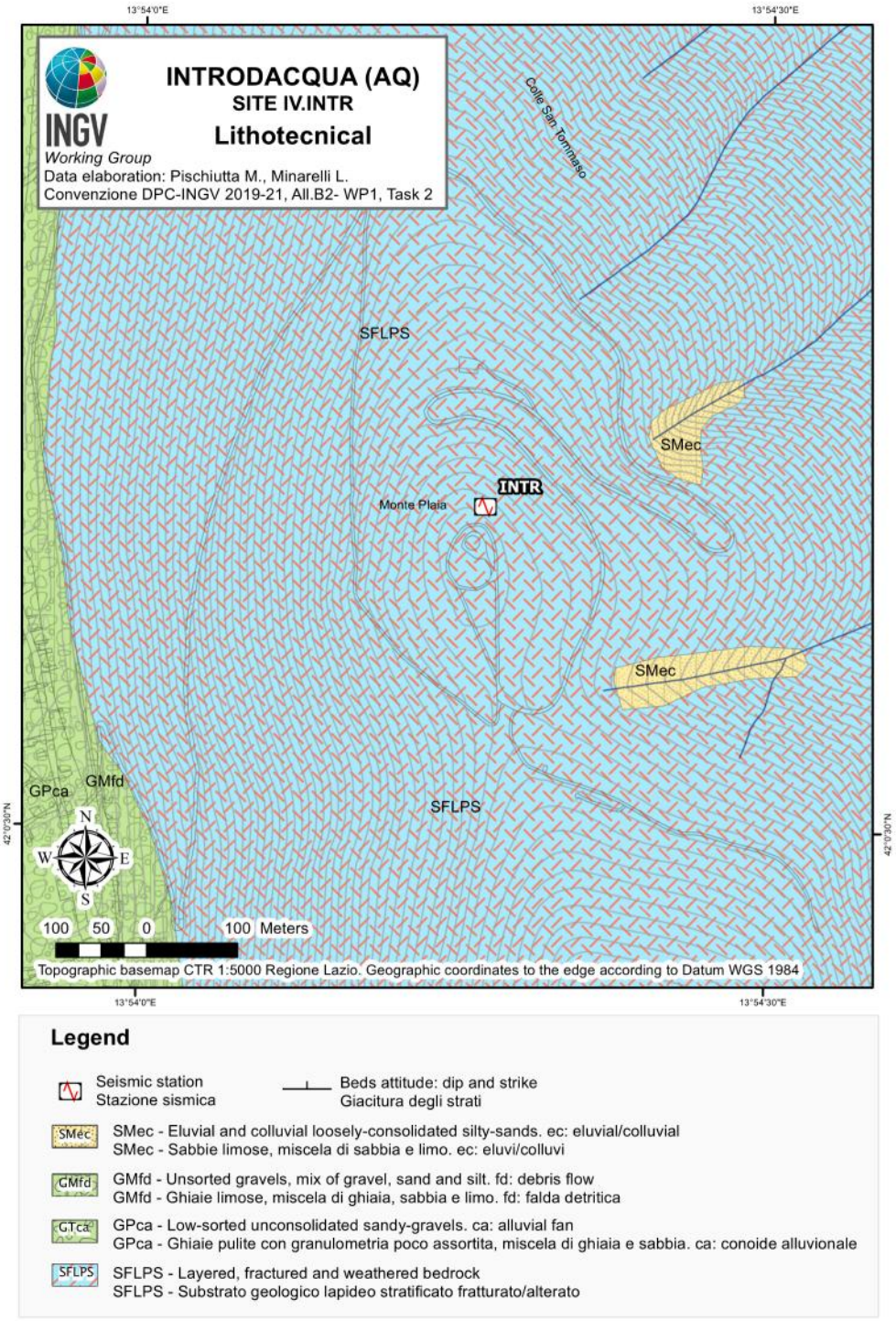


**Figure 2:** Lithotechnical map of the seismic station IV.INTR, scale 1:5.000. The lithotechnical units are deduced from the Geological map of Italy sheets 369 (Sulmona), scale 1:50.000, and assigned according to the nomenclature of Seismic Microzonation (Technical Commission SM, 2015).

## A4. SURVEY MAP

Figure 3 shows the Survey Map reporting both previous investigations and geophysical surveys conducted by INGV Working Group.

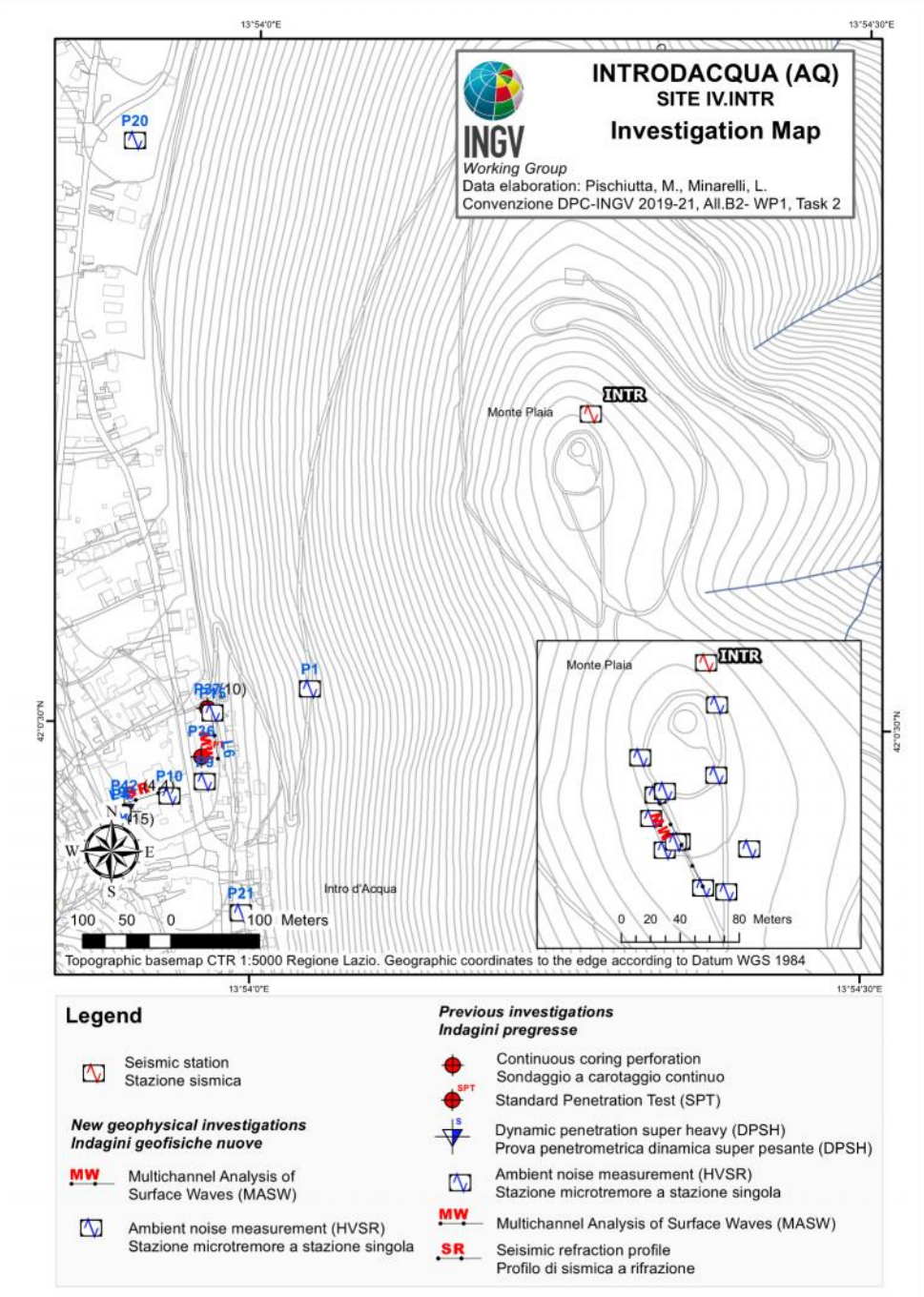


**Figure 3:** Map of the surveys in the surroundings of the station IV.INTR, scale 1:5.000. The box at the bottom right contains a zoom of the area with the details of the geophysical survey conducted by INGV Working Group for the seismic characterization of the site (Agreement DPC-INGV 2019-21, All. B2, WP1 - TASK 2, Velocity profile report IV.INTR)

## A5. GEOLOGICAL MODEL

### A5.1 General description

The seismic station is installed on Monte Plaia, an 850m-high topography with geometry roughly 2D, steep slopes (20 to 35°), and elongated in N-S direction. It is located in the eastern sector of the central Apennines, a thrust-fold belt with north-east vergence. In the studied area, tectonic structures involved Triassic-Miocene carbonates belonging to the Lazio-Abruzzi domain, in particular to the *Prezza tectonic Unit* (Figure 4, left panel), as defined in the Notes attached to the Geological Map of Italy (sheet 365, Sulmona). This latter is part of *Gran Sasso-Genzana* tectonic unit, which was thrusted with Adriatic vergence over the *Laga-Queglia* tectonic unit. *Prezza tectonic Unit* includes a northern sector with compressive structures oriented mainly E-W, and an eastern one with prevailing N-S structures. All these tectonic units are composed of carbonatic lithotypes belonging to the Laziale-Abruzzese carbonate platform domain and transition basins. In the *Prezza Unit*, upon the carbonate inner platform facies in the Calcare Massiccio Unit (lower Lias),distal-slope to basin successions are deposited (Jurassic-Cretaceous) passing to slope (lower Cretaceous) and upper to mid-outer ramp deposits (Paleogene-Miocene). From the stratigraphic point of view, the studied area is included in the "*Sagittario Popoli Gizio*" area (D), as evidenced by Figure 4 (right panel).

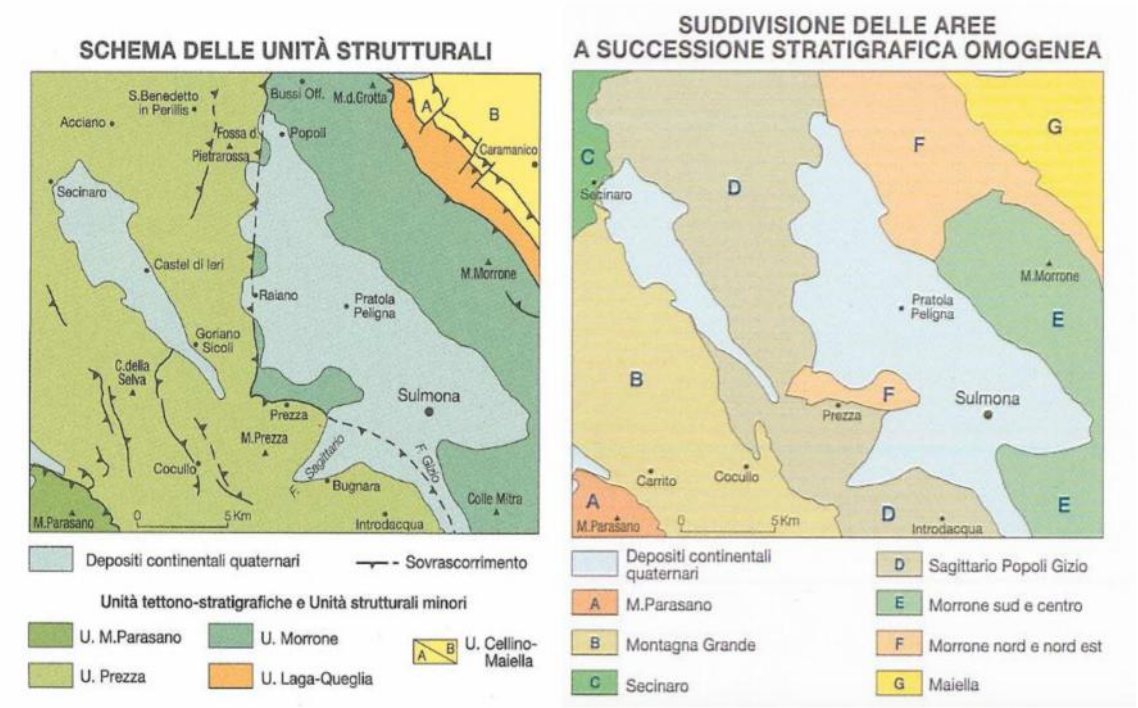


**Figure 4:** Classification adopted in the Geological Map, scale 1:50.000 (sheet 365-Sulmona), grouping tectonic units (left panel), and lithostratigraphic units with homogeneous stratigraphic sequence (right panel).

In this sector of the Apennines, the construction of the thrust-fold belt started from upper Messinian, progressively continuing towards East until middle Pliocene-lower Pleistocene. In the Upper Pliocene inner thrust were locally reactivated.
The entire chain was dislocated by Quaternary normal trastensive faults with NW-SE strike (from NNW-SS, to N-S, and E-W), often reactivating pre-existing structures (thrust, normal or strike-slip). Such faults are associated to morphological tectonic depressions and intermontane sedimentary basins, as well to an intense seismic activity.
Thus, morphology evolution was strictly controlled by this latter tectonic activity, affecting the area since the lower to middle Pleistocene. The relief is mainly elongated in NW-SE direction, delimiting sedimentary basins filled by Quaternary sediments. The morphology in the studied area is also dominated by a large alluvial fan, originated from the southern relief of Monte Genzana.
The geological bedrock consists of marine carbonate sedimentary sequences deposited from Jurassic to Cretaceous, represented by fossil-rich calcarenites and calcirudites related to distal-slope to basin successions (Jurassic-Cretaceous) passing to slope (lower Cretaceous). In the studied area, they are involved in a NW-SE vergent anticline, whose eastern flank is exposed in Monte Plaia, stratification showing a regular attitude with N120-140 strike and 30° plunge.
In the area also debris flow and quaternary superficial eluvium deposits outcrop, both derived from weathering and erosion of bedrock limestones. They consist of unsorted gravels and loosely-consolidated silty sands, respectively.
Finally, in the southeastern sector of the studied area there is also evidence of a superficial slow rockslide, caused by widespread washout processes interesting the superficial portion of the carbonatic topography. It was recognized to be related to moderate risk by “Piano di Assetto Idrogeologico della Regione Abruzzo”, and to a low probability to be reactivated.

### A5.2 Geological Section

The seismic station is located on the top of Monte Plaia, an 860m-high hill with steep slopes. The geological cross section and the subsoil model (Figure 5) accompanying geological survey map provide an interpretation of the third dimension. The geological section was redrawn on the basis pre-existing geological studies.

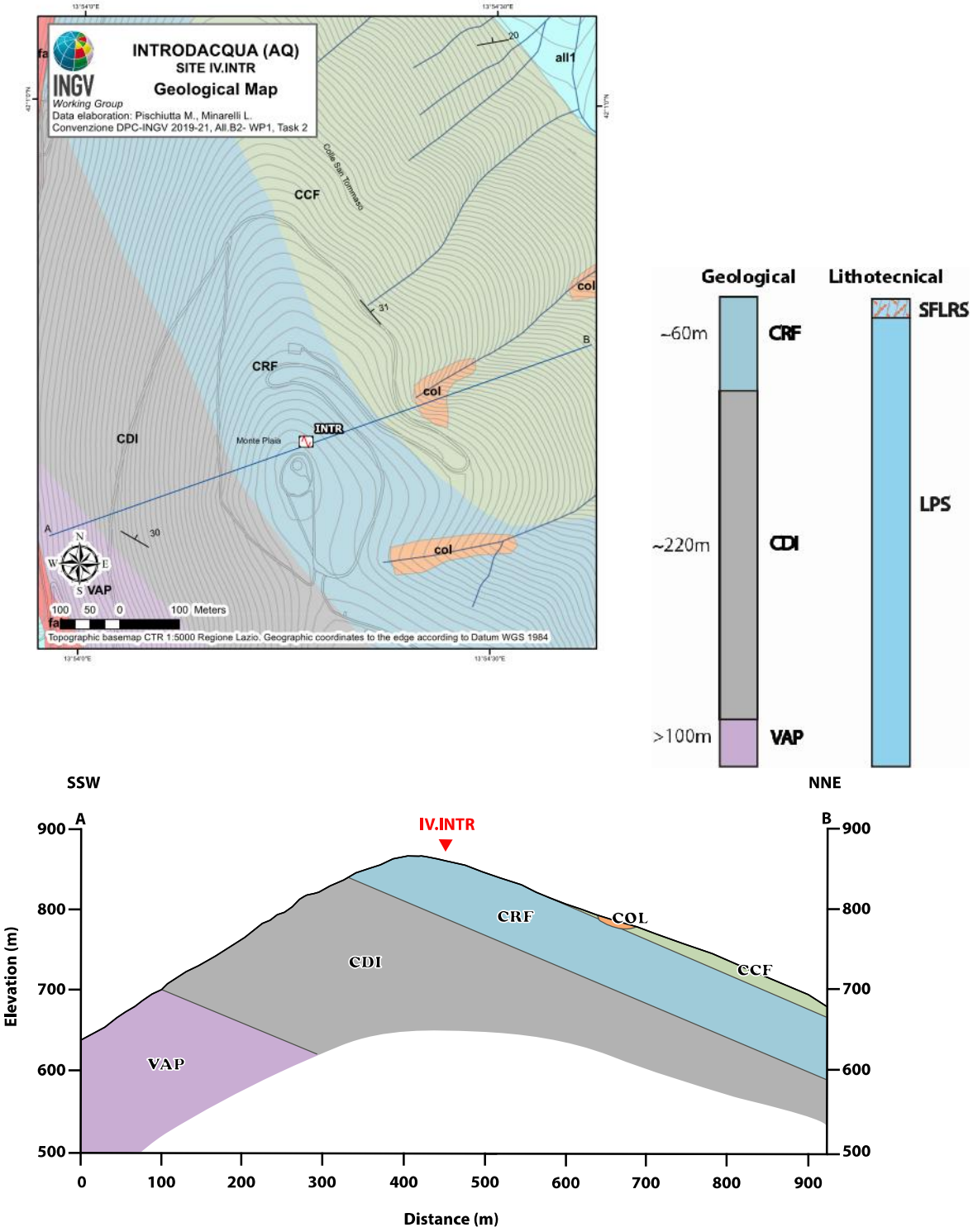


**Figure 5**. (left-top) Geological map of the study area where seismic station IV.INTR is installed indicating the trace on the map of the geological section; (right-top) subsoil model under IV.INTR seismic station and classification according to nomenclature in the Geological Map of Italy; (bottom) geological section passing through the site.

### A5.3 Subsoil model

There are not boreholes in the surroundings of the seismic station thus the subsoil model is based on the extrapolation of surface data, existing geological surveys, and new geophysical investigations, performed by the INGV Working Group, for the seismic characterization of the site and the definition of the velocity profiles of the body waves.

Mt Plaia hill, where station IV.INTR is installed, is entirely composed of marine carbonate sedimentary sequences deposited from Jurassic to Cretaceous, and represented by fossil-rich calcarenites and calcirudites related to distal-slope to basin successions (Jurassic-Cretaceous). As shown by the Geological Map (sheet 365 Sulmona), the youngest outcropping unit in the studied area is represented by *Calcareniti e calciruditi a Fucoidi Fm*. (CCF), composed of two distinct members (Aprian-Cenomanian). The lower one is represented by bioclastic rudstones and grainstones in thick to mid layers, with pebble elements (dimensions from cm to dm), Rudista fragments and sharp-edged flint. The upper member is composed of bioclastic packstones and rudstones in mid to thick layers, with lenticular pebble elements in a bioclastic matrix made of highly-fragmented Rudista.

The next Unit is indicated as CRF, *Calcareniti a radiolari e resti filamentosi Fm*. (Upper Jurassic) with thickness ranging from 100 to 400m, and constituted of mudstones, wakestones with filaments and packstones with ooides and peliods, deposed in proximal basin and outer ramp conditions, in thick to mid strata, also showing grey flint intercalations (Titonian). CRF passes above to *Calcari Diasprini detritici Fm.* (CDI), with thickness varying from 30 to 100m and represented by bioclastic packstones with oolites and peloids in mid layers, and by mudstones and wackestones in thin to mid layers.

Finally, the lower Unit is represented by *Verde Ammonitico Fm*., with thickness from few to tens of meters. It is composed of clayey and calcareous marls, bioclastic packstones, mudstones and wavestones in mid thin layers, rich of filaments. In the lower part this unit is rich of rests of Ammonites and traces of bioturbation (Toarcian Bathonian).

The above-described sedimentary units are all involved in the eastern flank of an anticline, with axis striking in N-S direction, approximately. Strata thickness below the seismic station was extrapolated considering beds attitude as measured on rock outcrops (about 120-140 strike and 30° plunge) as follows: CRF 60 m; CDI 220-230m; VAP more than 100m.

| | |
|---|---|
| VAP | Verde ammonitico Fm. (Middle Jurassic) |
| CDI | Calcari diasprigni detritici Fm. (Upper Jurassic) |
| CRF | Calcareniti a radiolari e resti filamentosi Fm. (Upper Jurassic) |
| CCF | Calcareniti e calciruditi a fucoidi Fm. (Middle Cretaceous) |

# B. Vs profile

## B1. GEOPHYSICAL INVESTIGATIONS

We performed various geophysical investigations in the area around the IV.INTR seismic station, with the aim of determining a 1D-velocity model representing the subsoil underlying the seismic station. We carried out a MASW survey by using 72 vertical geophones deployed in linear configuration and, in addition, we installed 11 temporary seismic stations to record ambient noise. Figure 1 shows the location of linear array and of temporary seismic stations deployed in the target area near to the IV.INTR station (red triangle).

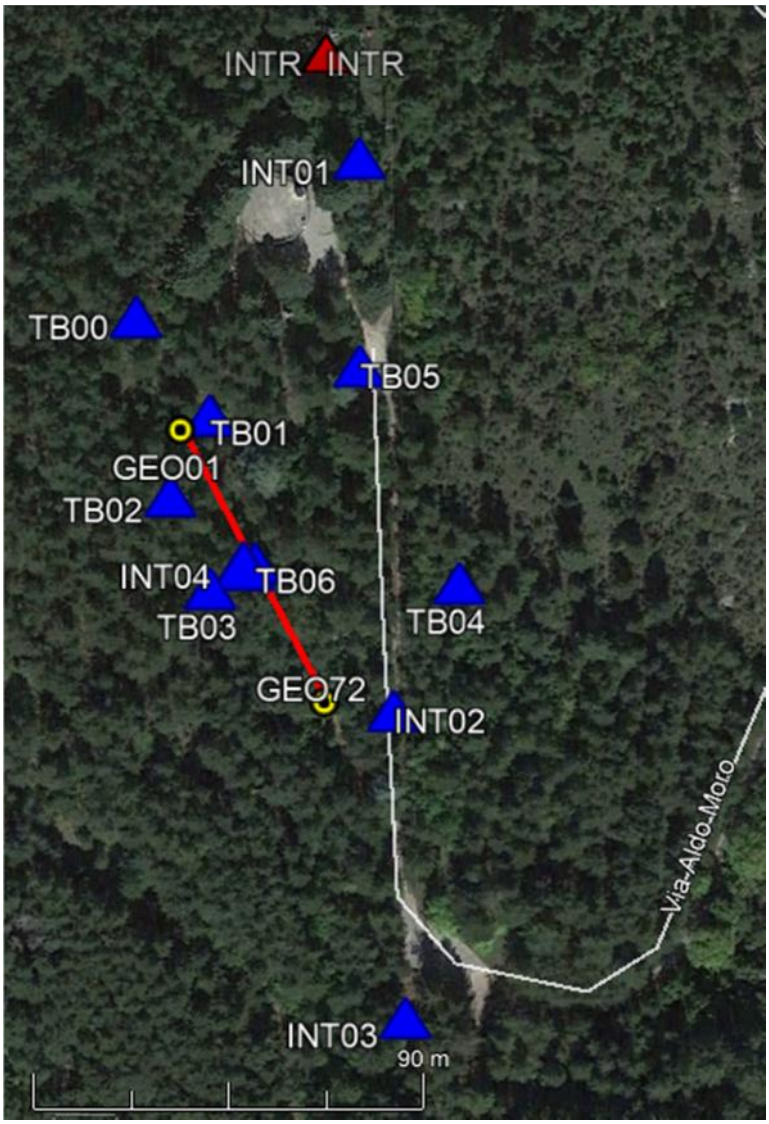


**Figure 6**. Plan view of the linear array (red line) and temporary seismic stations (blue triangles) located on Mount Plaia (Introdacqua, AQ), near the IV.INTR permanent seismic station (red triangle).

Due to the rugged topography and the dense vegetation in the area around the station, the geophysical surveys were conducted in an area more favorable to the installation located in the southern part of the station. For the linear array we used a dirt road that led to a disused restaurant. The MASW survey was performed using the data acquired by 72 vertical geophones (with natural frequency of 4.5 Hz) equally spaced of 1 m. Seismic noise was acquired by 11 seismic stations: 7 Terrabot (named as TB0X in Figure 6) station (made by Sara srl) equipped with tri-axial geophones (having 4.5 Hz as natural frequency) and a 24 bit digitizer; 4 stations composed by a Lennartz-5s sensor coupled to a Reftek130 digitizer (named as INT0X in Figure 6). Measurements were acquired on 17 September 2020 when we benefited of favorable weather conditions (sunny day without wind). Figure 7 shows some pictures taken during the performed measurements.


**Figure 7**. Pictures taken during the measurements day: (left) site hosting the IV.INTR seismic station; (middle) linear array; (right) examples of temporary seismic stations in ambient noise acquisition on 17 September 2020.

### B1.2 HV noise spectral ratios

The temporary seismic stations acquired data for about 3 hours that were used to compute the H/V spectral ratios at different station sites. Figure 8 shows the H/V computed for all the 11 stations. There is a good agreement of the H/V shapes and amplitudes showing a good matching in the investigated frequency range. This is also confirmed by Figure 9, where we superimpose all the mean H/V curves. At all measuring sites we consistently observe a clear peak between 1 and 3 Hz. However, there is a variation between stations in the frequency values associated with the maximum amplitude. Frequency values ($f_0$) vary from 1.3 Hz (at INT01 station) to 1.7

Hz (at TB03 and INT03 stations). At stations INT01, INT02, INT04, TB01, TB02, TB03, TB04 the H/V peak seems to be composed by two different semi-superimposed peaks (Figure 8 and Figure 9).

Figure 9c shows the areal distribution of frequency peaks at different stations, suggesting a decrease of frequency peak moving from south to north.

For all of the measurement sites, the rotated H/V spectral ratios evidence a coherent polarization effect (Figure 10). Results highlight a relevant directional amplification effect with maximum amplification along N160° direction. This is consistent with findings by Pischiutta et al. (2018) who investigated H/V spectral ratios using both ambient noise and earthquake recordings at station IV.INTR. They found a single frequency peak at 1.7 Hz (on ambient noise) and at 1.2 (on earthquake recordings), with amplitudes up to a factor of 3.8 and maximum amplification in N150° direction.

Considering the information collected so far, as well as the absence of a deep stratigraphic log, in this stage we exclude that this peak between 1 and 2 Hz could be caused by a stratigraphic effect with a velocity contrast at depth. In fact, the geological subsoil model (see Figure 5) does not suggest the presence of stratigraphic contrasts, being characterized by an almost-continuous stratigraphic succession of carbonate rocks.

Unfortunately in the case of IV.INTR station it is difficult to explain the observed directional effect using simple resonant topography model (e.g. Spudich et al., 1996; Pischiutta et al. 2018), since the maximum amplification of the H/V ratios occurs in a direction that is almost parallel to the main hill elongation.

The interpretation of the patterns of the H/V curves needs to be thorough studied in further investigations, that are beyond the goal of the present report.

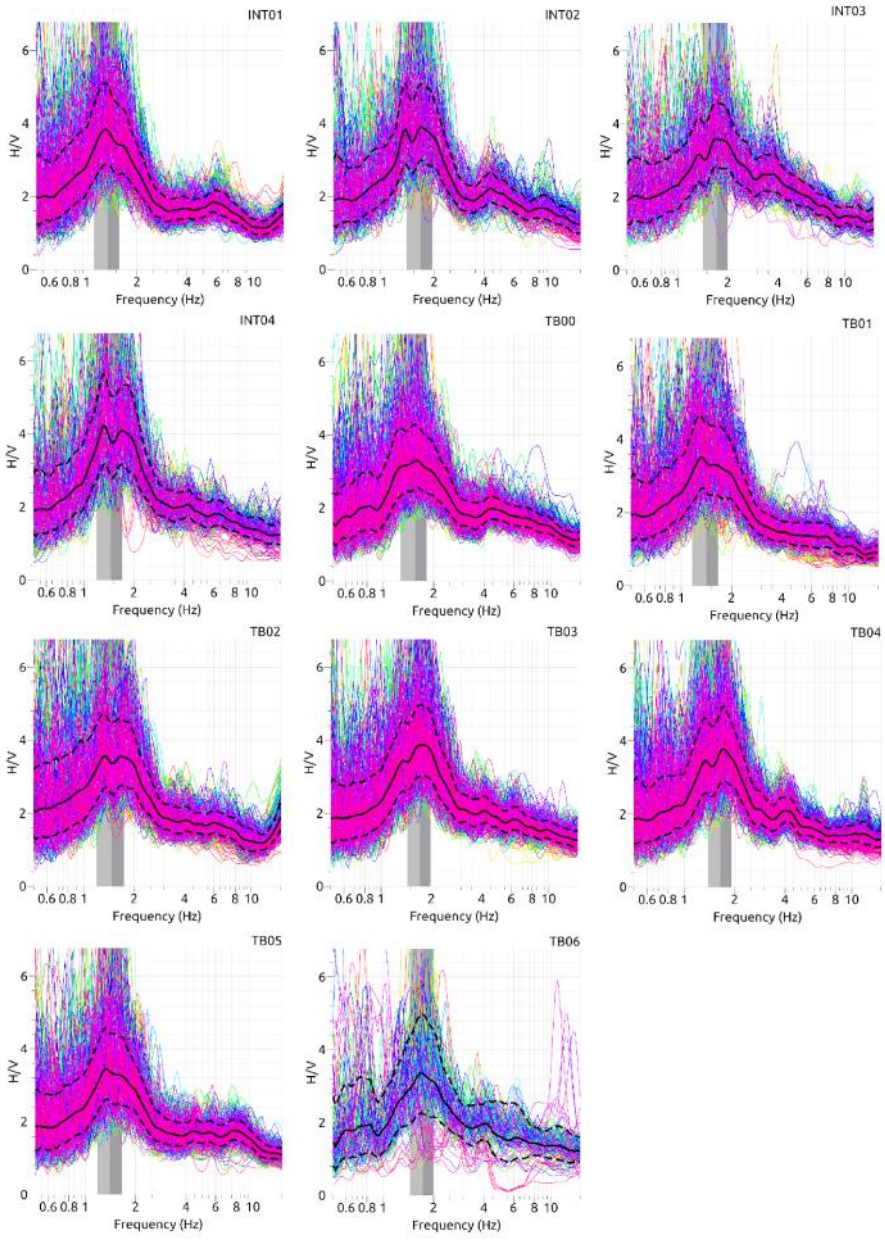


**Figure 8**. Results of H/V analysis performed on data acquired at 11 seismic stations installed during the geophysical survey. For each result, the related station is shown at the top right of the figure.

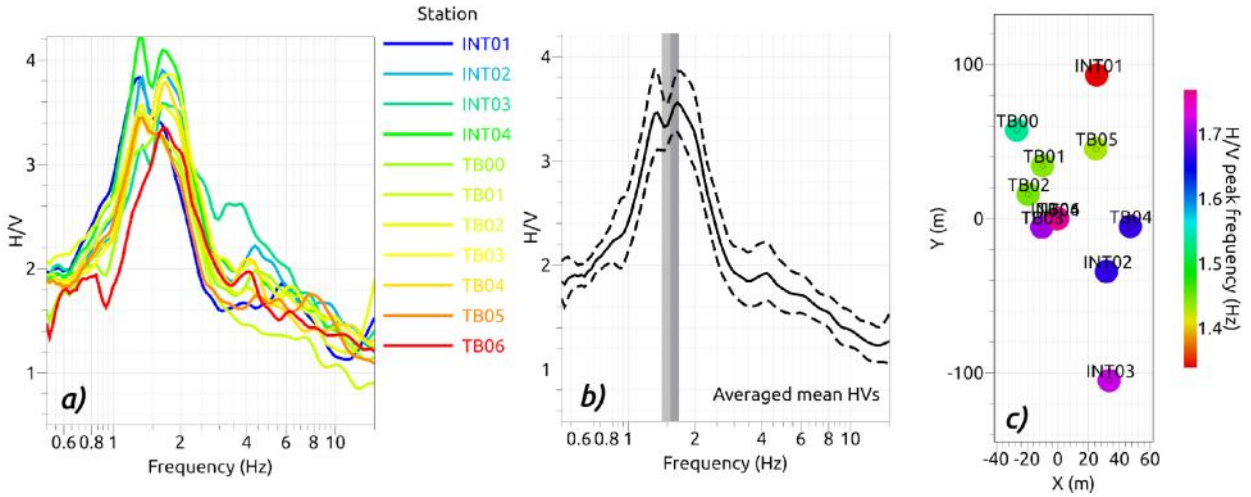


**Figure 9**. Mean H/V curves of the 11 stations (a). H/V curve determined using the results obtained at all stations (b). Areal distribution of $f_0$ at 11 stations (c).

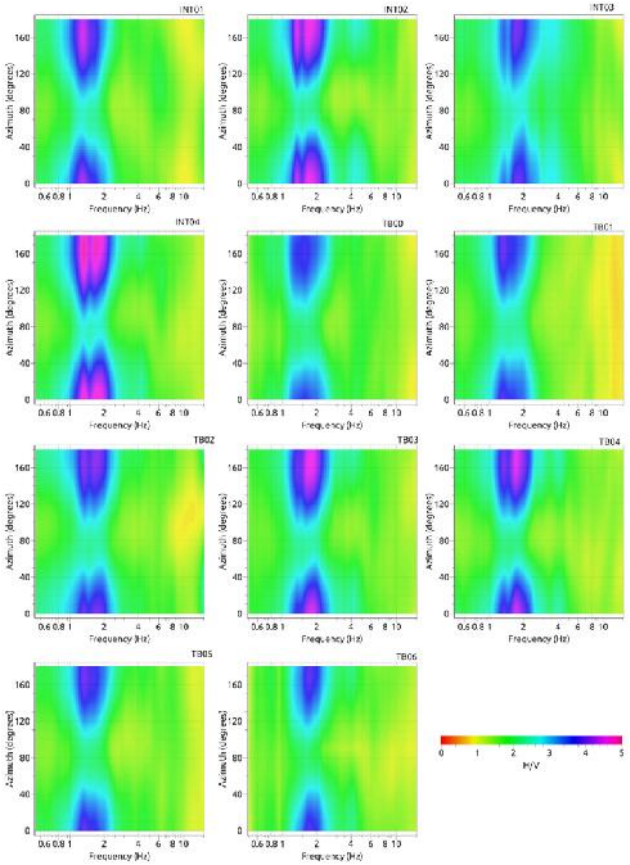

**Figure 10**. H/V spectral ratios obtained after rotating the two horizontal components by steps of 10°, from 0° to 180°. We show results obtained at all the 11 stations (the related name is shown at the top right of each sub-figure).

### B1.3 Dispersion curves from linear array

The 72 vertical geophones were deployed along a straight line and were equally spaced of 1 m. For the MASW analysis, we acquired the seismic signals produced by the impact of a 5 kg hammer on the ground. The shots were made along the line at distances (offset) of -10 m, -5 m, -2 m, 34.5 m, 73 m, 76 m and 81 m from the position of the first geophone (GEO01 in Figure 6 considered at 0 m). In each shot point, the measurements were repeated three times (four times for the shot at 73 m) in order to increase data redundancy, thus trying to better verify the results obtained. The seismic data were acquired using three multi-channels systems (Geode manufactured by Geometrics, each of which manages 24 channels) with a sampling rate of 0.125 ms for a duration of 2 s.

The acquired data were processed using the *GEOPSY* software tools (www.geopsy.org) in order to extract the surface-wave dispersion properties of subsoil by applying frequency-wavenumber (FK) transform to the seismic signals. Figure 11 shows the results obtained with the linear active survey (MASW).

We identified a dispersion curve for the shots located at the following distances from the first geophone: -10 m; -5 m; 73 m; 76 m and 81 m. The picking of these dispersion curves was carried out manually (black lines in Figure 11). Unfortunately, for the shots located at – 2 m and 34.5 m we obtained low-quality results and it was not possible to pick any dispersion curves.

In order to obtain a new dispersion curve in a complementary way respect to the MASW technique, the seismic noise recorded at the geophones of the linear array (about one hour of signal at 250 sps) were cross-correlated between the different pairs of stations and the results were analyzed through a Constant Velocity Stack analysis (CVS, Vassallo et al. 2019). Figure 12 shows the results of CVS analysis performed on cross-correlation functions and the related dispersion curve (black line). The results obtained from the cross-correlation analysis are consistent with those derived from the MASW, and allowed us to extract information on the dispersion towards lower frequencies, reaching 10 Hz.

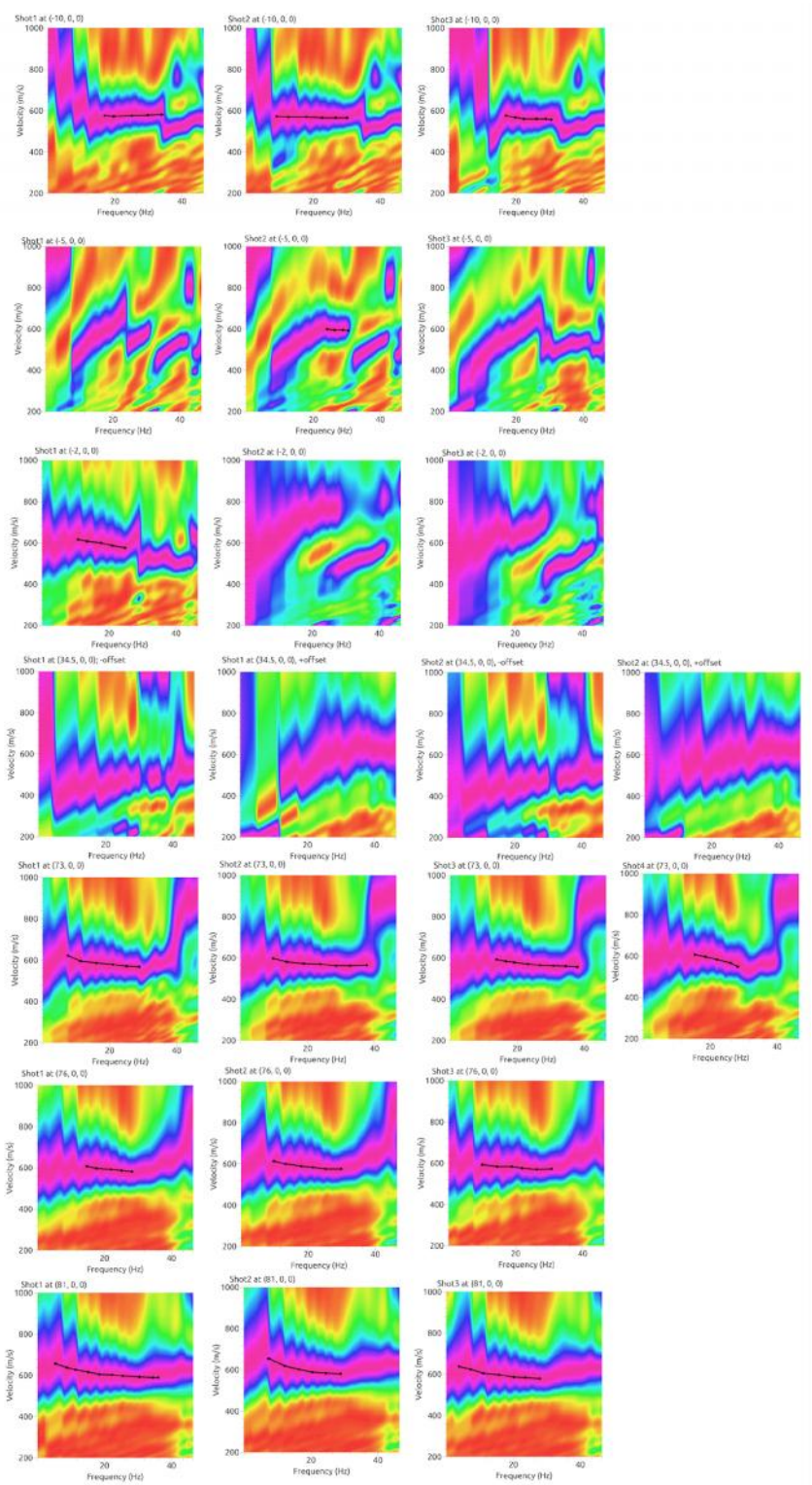

**Figure 11.** FK analysis. The results obtained by MASW analysis are shown for each shot; from top to down the offset is -10 m, -5 m, -2 m, 34.5 m, 73 m, 76 m and 81m. Plots in the same horizontal panel refer to the same shot offset location and the black curves lines represent the picked dispersion curve.

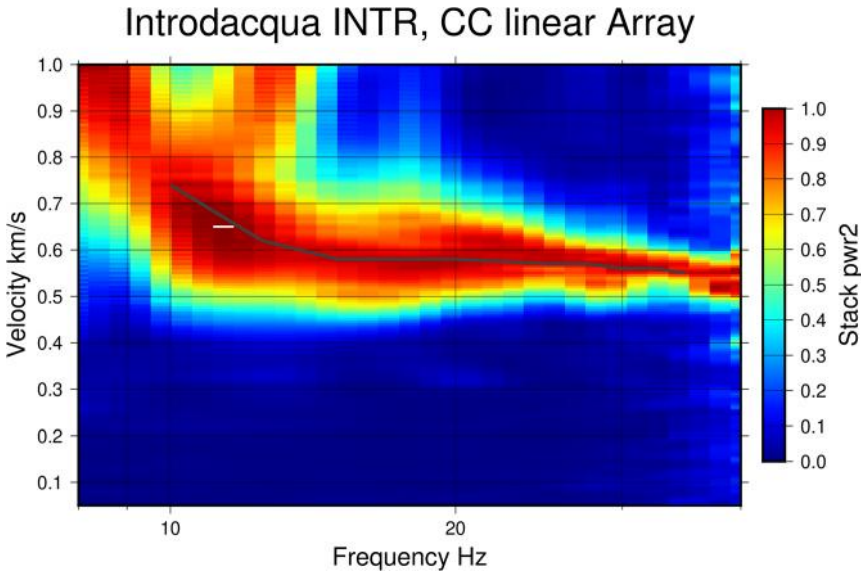


**Figure 12.** Results obtained by Constant Velocity Stack analysis performed on cross-correlation functions computed on passive data from geophones pairs of linear array. The black line represents the picked dispersion curve.

## B2. Seismic Velocity Model

Figure 13 reports all the extracted dispersion curves (and related uncertainties) from the linear array of geophones. We combined all the picked dispersion curves from MASW and cross-correlation analysis in order to obtain the final dispersion curve used as target in the inversion procedure (the red curve of Figure 13).

To proceed with the inversion step, the dispersion curve derived from the vertical component of motion was associated with the fundamental mode of surface Rayleigh-wave. Then, we inverted through the *GEOPSY* tool the apparent surface-wave dispersion curve for recovering the shear-wave velocity (Vs) model. We chose not to perform a join inversion of the dispersion and the H/V curve. In fact, the results from H/V analysis (polarization and areal distribution of peak frequencies) suggest that the amplification peaks at the measurement sites is not attributable to a stratigraphic effect with a velocity contrast at depth. Moreover, the geological subsoil model does not suggest the presence of stratigraphic contrasts, being characterized by an almost-continuous stratigraphic succession of carbonate rocks (see Figure 5).

The resulting velocity models obtained from the inversion of the dispersion curve are shown in Figure 14. We tested several simple starting model-parameterization composed of different uniforms and linear velocity increase (with depth) layers over half-space, keeping in mind the limited depth of maximum investigation associated with our dispersion curve (in the range 23-35 m). The best Vp and Vs models (i.e. lowest misfit) resulting from the inversion are shown in Figure 15 and Table 1.

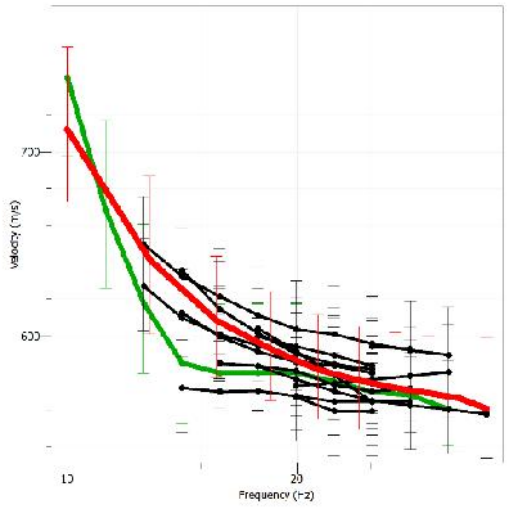


**Figure 13.** Manually-picked dispersion curves from the results of MASW (black lines) and CVS on cross-correlation data (green line). The red line shows the dispersion curve determined using all the manually picked dispersion curves. The red curve is used as input data of inversion procedure.

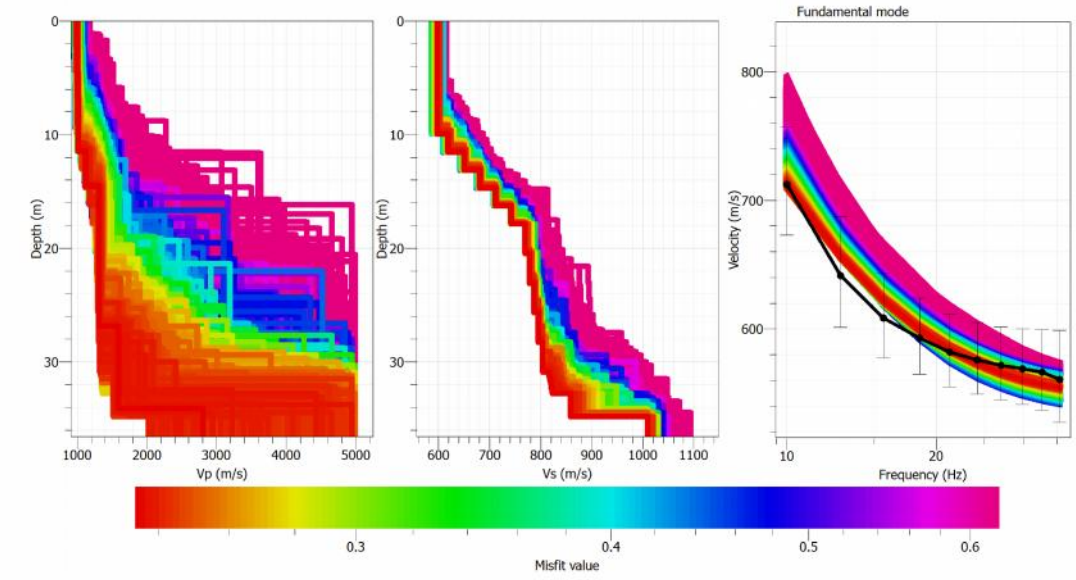


**Figure 14.** Models derived from the inversion of the experimental dispersion curve. Vp models on the left, Vs models in the middle and theoretical dispersion curves on the right (the experimental dispersion is shown in black). The color scale is proportional to the misfit between experimental curve and theoretical models. The best Vp and Vs model (i.e. lowest misfit) are presented in Figure 15.

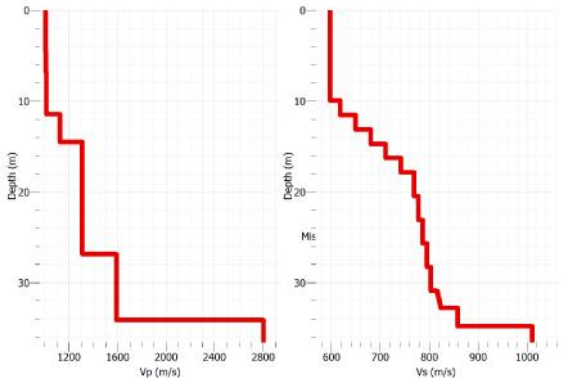


**Figure 15.** Best Vp and Vs models (among the models shown in Figure 15) obtained after the inversion of the experimental apparent surface-wave Rayleigh dispersion curve.

**Table 1**. Best-fit model

| From (m) | To (m) | Thickness (m) | Vp (m/s) | Vs (m/s) |
|---|---|---|---|---|
| 0 | 2.29 | 2.29 | 1005.1 | 597.6 |
| 2.29 | 4.58 | 2.29 | 1007.1 | 597.6 |
| 4.58 | 6.87 | 2.29 | 1009.1 | 597.6 |
| 6.87 | 9.16 | 2.29 | 1011.1 | 597.6 |
| 9.16 | 9.96 | 0.8 | 1013.1 | 597.6 |
| 9.96 | 11.45 | 1.49 | 1013.1 | 618.9 |
| 11.45 | 11.54 | 0.09 | 1126.8 | 618.9 |
| 11.54 | 13.12 | 1.58 | 1126.8 | 649.7 |
| 13.12 | 14.5 | 1.38 | 1126.8 | 680.5 |
| 14.5 | 14.72 | 0.21 | 1308.2 | 680.5 |
| 14.71 | 16.29 | 1.58 | 1308.2 | 711.3 |
| 16.29 | 17.87 | 1.58 | 1308.2 | 742.1 |
| 17.87 | 20.47 | 2.61 | 1308.2 | 769.4 |
| 20.47 | 23.08 | 2.61 | 1308.2 | 778 |
| 23.08 | 25.68 | 2.61 | 1308.2 | 786.5 |
| 25.68 | 26.88 | 1.19 | 1308.2 | 795.1 |
| 26.88 | 28.29 | 1.41 | 1592.3 | 795.1 |
| 28.29 | 30.9 | 2.61 | 1592.3 | 803.7 |
| 30.9 | 31.28 | 0.38 | 1592.3 | 816.9 |
| 31.28 | 31.66 | 0.38 | 1592.3 | 818.5 |
| 31.66 | 32.04 | 0.38 | 1592.3 | 820.2 |
| 32.04 | 32.43 | 0.38 | 1592.3 | 821.8 |
| 32.42 | 32.8 | 0.38 | 1592.3 | 823.4 |
| 32.8 | 34.14 | 1.33 | 1592.3 | 858.5 |
| 34.14 | 34.83 | 0.7 | 2805.2 | 858.5 |
| 34.83 | | --- | 2805.2 | 1010 |

## B3. Conclusion

Surface-wave analysis at IV.INTR station indicates that the site can be related to soil class-B, as prescribed in the italian seismic design codes NTC-18 and NTC-08, and in the EC8 (Table 2). The best Vp and Vs models (i.e. lowest misfit) resulting from the inversion are shown in Figure 15 and Table 1.
H/V noise spectral ratios of the temporary stations installed during the survey, show a clear peak between 1 and 3 Hz, with peak frequencies $f_0$ varying from 1.3 Hz to 1.7 Hz. We also observe that maximum amplification occurs along N160° azimuth, consistently with findings by Pischiutta et al. (2018), who investigated H/V spectral ratios using both ambient noise and earthquake recordings at station IV.INTR.
The active linear array of geophones provided a final dispersion curve from 10 Hz to 35 Hz (Figure 13), and the inversion procedure resulted in the Vs models of Figure 14 and 15 where the bottom bedrock layer is found at a depth of 28.3 m (Table 1).
The $V_{S30}$ retrieved from the best inverted model is 661 m/s (Table 2), therefore IV.INTR is classified following EC8 or NTC08 as soil class B. Following the definition of $V_{S,eq}$ within NTC18, since the value of 800 m/s is reached at a depth of 28.3 m, $V_{S,eq}$ is equal to 630 m/s and the site can be related to class B.
We highlight that this site was previously related to class A in the Itaca database, where in absence of direct velocity measurements the site classification was assigned only considering the outcropping lithotypes.
Further investigations will be needed also to explore the presence of faults and fractured rocks which could affect the observed amplification pattern. However, they are beyond the goal of the present study.

**Table 2**. $f_0$ value, and soil class following NTC08 and NTC18.

| **$f_0$ (Hz)** | **Note** |
|---|---|
| 1.6 Hz | The H/V peak is polarized along N160° direction. |

| **$V_{S30}$ (NTC08 or EC8)** | **Soil Class** |
|---|---|
| 661 m/s | B |

| **$V_{S,eq}$ (NTC18)** | **Soil Class** |
|---|---|
| 630 m/s | B |

## REFERENCES

EC8: European Committee for Standardization (2004). Eurocode 8: design of structures for earthquake resistance. P1: General rules, seismic actions and rules for buildings. Draft 6, Doc CEN/TC250/SC8/N335.

Geological Map of Italy, scale 1:100.000 (1943) - Sheet 146 - Sulmona. ISPRA http://193.206.192.231/carta_geologica_italia/tavoletta.php?foglio=146

Geological Map of Italy, scale 1:50.000 (2005) - Sheet 369 - Sulmona. ISPRA http://www.isprambiente.gov.it/Media/carg/369_SULMONA/Foglio.html

NTC 2018: Ministero delle Infrastrutture e dei Trasporti (2018). Aggiornamento delle Norme Tecniche per le Costruzioni. Part 3.2.2: Categorie di sottosuolo e condizioni topografiche, Gazzetta Ufficiale n. 42 del 20 febbraio 2018 (in Italian).

PAI Piano Stralcio di Bacino per l'Assetto Idrogeologico dei Bacini Idrografici di Rilievo Regionale Abruzzesi e del Bacino Interregionale del Fiume Sangro "Fenomeni Gravitativi e Processi Erosivi", http://autoritabacini.regione.abruzzo.it/index.php

Pischiutta, M., P. Cianfarra, F. Salvini, F. Cara, and P. Vannoli (2018). A systematic analysis of directional site effects at stations of the Italian seismic network to test the role of local topography, Geophys. J. Int. 214(1) 635–650. https://doi.org/10.1093/gji/ggy133

Spudich, P., Hellweg, M. & Lee, W.H.K., 1996. Directional topographic site response at Tarzana observed in aftershocks of the 1994 Northridge, California, earthquake: implications for mainshock motions, Bull. seism. Soc. Am., 86, S193–S208.

Technical Commission SM, 2015 – Microzonazione sismica. Standard di rappresentazione e archiviazione informatica, Versione 4.0b (Commissione tecnica inter-istituzionale per la MS nominata con DPCM 21 aprile 2011).

Vassallo, M., R. De Matteis, A. Bobbio, G. Di Giulio, G. M. Adinolfi, L. Cantore, R. Cogliano, A. Fodarella, R. Maresca, S. Pucillo and G. Riccio, (2019). Seismic noise cross-correlation in the urban area of Benevento city (Southern Italy). GEOPHYSICAL JOURNAL INTERNATIONAL, vol. 217, pp. 1524–1542, 2019. https://doi.org/10.1093/gji/ggz101

***Disclaimer and limits of use of information***

*The INGV, in accordance with the Article 2 of Decree Law 381/1999, carries out seismic and volcanic monitoring of the Italian national territory, providing for the organization of integrated national seismic network and the coordination of local and regional seismic networks as described in the agreement with the Department of Civil Protection.*

*INGV contributes, within the limits of its skills, to the evaluation of seismic and volcanic hazard in the Country, according to the mode agreed in the ten-year program between INGV and DPC February 2, 2012 (Prot. INGV 2052 of 27/2/2012), and to the activities planned as part of the National Civil Protection System. In particular, this document[1] has informative purposes concerning the observations and the data collected from the monitoring and observational networks managed by INGV.*

*INGV provides scientific information using the best scientific knowledge available at the time of the drafting of the documents produced; however, due to the complexity of natural phenomena in question, nothing can be blamed to INGV about the possible incompleteness and uncertainty of the reported data.*

*INGV is not responsible for any use, even partial, of the contents of this document by third parties and any damage caused to third parties resulting from its use.*

*The data contained in this document is the property of the INGV.*

***Esclusione di responsabilità e limiti di uso delle informazioni***

*L'INGV, in ottemperanza a quanto disposto dall'Art. 2 del D.L. 381/1999, svolge funzioni di sorveglianza sismica e vulcanica del territorio nazionale, provvedendo all'organizzazione della rete sismica nazionale integrata e al coordinamento delle reti sismiche regionali e locali in regime di convenzione con il Dipartimento della Protezione Civile.*

*L'INGV concorre, nei limiti delle proprie competenze inerenti la valutazione della Pericolosità sismica e vulcanica nel territorio nazionale e secondo le modalità concordate dall'Accordo di programma decennale stipulato tra lo stesso INGV e il DPC in data 2 febbraio 2012 (Prot. INGV 2052 del 27/2/2012), alle attività previste nell'ambito del Sistema Nazionale di Protezione Civile.*

*In particolare, questo documento[1] ha finalità informative circa le osservazioni e i dati acquisiti dalle Reti di monitoraggio e osservative gestite dall'INGV.*

*L'INGV fornisce informazioni scientifiche utilizzando le migliori conoscenze scientifiche disponibili al momento della stesura dei documenti prodotti; tuttavia, in conseguenza della complessità dei fenomeni naturali in oggetto, nulla può essere imputato all'INGV circa l'eventuale incompletezza ed incertezza dei dati riportati.*

*L'INGV non è responsabile dell'utilizzo, anche parziale, dei contenuti di questo documento da parte di terzi e di eventuali danni arrecati a terzi derivanti dal suo utilizzo.*

*La proprietà dei dati contenuti in questo documento è dell'INGV.*



[1]This document is level 3 as defined in the "Principi della politica dei dati dell'INGV (D.P. n. 200 del 26.04.2016)"